"M1 macrophage subtypes activation and adipocyte dysfunction worsen during prolonged consumption of a fructose rich diet"

Gambaro SE[1]; Zubiria MG[1,2]; Portales A[1]; Rey MA[1]; Rumbo M[3]; Giovambattista A[1,2]

[1]Laboratorio de Neuroendocrinología, Instituto Multidisciplinario de Biología Celular (IMBICE, CICPBA-CONICET-UNLP), Calle 526, 10 y 11, La Plata 1900, Argentina;

[2]Departamento de Ciencias Biológicas, Facultad de Ciencias Exactas, Universidad Nacional de La Plata, 1900, Argentina.

[3]Instituto de Estudios Inmunológicos y Fisiopatológicos, CONICET-UNLP, La Plata

Corresponding author:

Dr. Andrés Giovambattista

agiovamba@imbice.gov.ar

Instituto Multidisciplinario de Biología Celular, IMBICE

526 y 11 S/N La Plata, Buenos Aires, Argentina

CP 1900 Tel: +54-221-4210112 int 219

Declarations of interest: none

Running title: "M1 subtypes and adipocyte hypertrophy increase with FRD"

Fundings: This work was supported by grants from Agencia Nacional de Promoción de la Ciencia y la Tecnología (PICT-2013-0930 and PICT-2015-2352).

Keywords: Fructose rich diet; adipose tissue hypertrophy; macrophages subtypes; adipocytes-macrophages crosstalk

Color figures only in printed version

Abstract

Fructose rich diet (FRD) has been associated with obesity development, which is characterized by adipocytes hypertrophy and chronic low-grade inflammation. Interaction of adipocytes and immune cells play a key role in adipose tissue (AT) alterations in obesity. We assessed the metabolic and immune impairments in AT in a murine obesity model induced by FRD at different periods. Adult Swiss mice were divided into groups of 6 and 10 weeks of fructose (FRD 6wk, FRD 10wk) or water intake (CTR 6wk, CTR 10wk). FRD induced increased in body weight, epidydimal AT mass, plasmatic and liver Tg, and impaired insulin sensitivity. Also, hypertrophic adipocytes from FRD 6wk-10wk mice showed higher IL-6 when stimulated with LPS and leptin secretion. Several of these alterations worsened in FRD 10wk. Regarding AT inflammation, FRD mice have increased TNFα, IL-6, IL1β, and decrease in IL-10, CD206 mRNA levels. Using CD11b, LY6C, CD11c and CD206 as macrophages markers, we identified for first time in AT M1 (M1a: Ly6C+/-CD11c+CD206- and M1b: Ly6C+/-CD11c+CD206+) and M2 subtypes (Ly6C+/-CD11c-CD206+). M1a phenotype increased from 6 weeks onward, while Ly6C+/- M1b phenotype increased only after 10 weeks. Finally, co-culture of RAW264.7 (monocytes cell line) and CTR or FRD adipocytes showed that FRD 10wk adipocytes increased IL-6 expression in non- or LPS-stimulated monocytes. Our results showed that AT dysfunction got worse as the period of fructose consumption was longer. Inflammatory macrophage subtypes increased depending on the period of FRD intake and hypertrophic adipocytes were able to create an environment that favored M1 phenotype in vitro.

1. Introduction

Worldwide incidence of obesity has reached dramatic levels, making it one of the main concerns for the public health system. World Health Organization (WHO) defines obesity as adipose tissue (AT) excess which may be harmful for health. AT excess is generated by the imbalance between calories intake and energy expenditure, where energy excess is stored mainly in AT, favoring its expansion. Obesity and overweight, especially abdominal fat accumulation, are major risk factors for a number of noncommunicable diseases including cardiovascular disorders, dyslipidemia, insulin resistance and certain cancers, among others [1–5].

Several factors, such as sedentary lifestyle and unbalanced diets, have converged to create the actual obesogenic environment. Regarding diets, high content of fat and sugar has been associated to detrimental effects on health. Thus, high fructose content in sweetened beverages has been associated to high prevalence of overweight and Metabolic Syndrome (MS)[6,7]. Besides, calories provided by sugar-sweetened beverages have little nutritional value and may not provide the same feeling of satiety as solid food. As an overall result, total energy intake increases, leading to unhealthy weight gain and co-morbidities (WHO). In animal models, fructose rich diet (FRD) has been related to the development of insulin resistance, dyslipidemias, increased abdominal AT mass, and changes in the pattern of AT adipokine secretion [8,9]. To some extent, these metabolic disorders are the consequence of fructose-induced hepatic de novo lipogenesis and the resulting increase in AT fatty acid uptake [10–12].

AT expansion implies tissue remodeling, which includes among others, the increase in number and size of adipocytes, and the recruitment and activation of immune cells. Hypertrophic adipocytes secrete more leptin and inflammatory cytokines, lower adiponectin and become insulin resistant [13]. Changes in the adipokine secretion pattern contribute to develop metabolic disorders and chronic low-grade inflammation, hallmark of obesity [14,15]. The AT inflammatory status plays a key role in the establishment of insulin resistance and AT macrophages (ATMs) are crucial for this process. It is known that macrophages may develop different phenotypes which play different roles in AT homeostasis. Using simplified criteria, the different populations of ATMs can be classified as classical (M1, pro-inflammatory) and alternative (M2, anti-inflammatory) activated macrophages. M1 macrophages are characterized by releasing IL-6, IL-1β, TNFα, and by having enhanced iNOS activity, while M2 macrophages are characterized by higher expression of IL-10 and arginase. In lean individuals,

resident ATMs mainly correspond to M2 type. Conversely, when chronic caloric excess persists and AT mass expansion is established, classical inflammatory ATMs are recruited and activated, leading to an increase in their number [16], while local proliferation and differentiation could contribute to the pathophysiological process [17].

Different monocyte/macrophage phenotypes have been described and are still a matter of debate. Monocytes can be characterized by the differential expression of an inflammatory marker Ly6C, being further divided as Ly6C^{+}(Ly6C^{high}+ Ly6C ^{middle}) and Ly6C^{-} (Ly6C^{low}). The first ones are more abundant in circulation, may be recruited into inflamed tissues and are capable to produce inflammatory cytokines when activated. In steady state, they may differentiate to Ly6C^{-} and become resident macrophages when they reach the tissue [18,19]. It is still controversial whether the latter ones may be activated to pro-inflammatory macrophages or to an intermediate phenotype. Moreover, CD11c has been widely used as a marker for M1 macrophages, while CD206 for M2 macrophages. A recent report has described the presence of CD206 marker in M1 ATMs splitting the M1 population into M1a for CD11c^{+} CD206^{-} cells and M1b for double positive CD11c^{+} CD206^{+} cells [20]. However, their origin and role in AT are still unknown.

A bi-directional interaction between adipocytes and ATMs has been widely studied and depending on the signals that both cellular types generate, they could modulate each other [21–23]. Adipocytes are capable to produce leptin, adiponectin, MCP-1, and pro-inflammatory cytokines, and may favor M1 or M2 ATMs, while cytokines derived from macrophages M1 and M2 impair or improve adipogenesis and insulin sensitivity, respectively.

For the present study we used a mouse model of fructose-induced obesity to assess the metabolic and inflammatory profile during two different periods: short FRD (6 weeks; FRD 6wk) and longer and chronic FRD (10 weeks; FRD 10wk). We mainly focused on the innate immune macrophage populations, M1 and subpopulations, M1a and M1b, and M2, with a novel set of markers CD11b, Ly6C, CD11c, and CD206. It is the first time that Ly6C marker is used to study ATM populations. Moreover, we studied the immune crosstalk between adipocytes and macrophages after the FRD.

2. Material and Methods

2.1. Animals and treatment

Normal adult male Swiss mice (four months of age) were kept in a temperature-controlled environment (20-22ºC, fix 12 h light/12 h dark cycles, lights on at 07:00 h) and fed *ad libitum*

with commercial rodent chow (Purina, Argentina). Mice were randomly group-housed: control animals were provided tap water for 6 or 10 weeks (CTR 6wk and CTR 10wk, respectively) or 20% fructose solution (wt/vol, Sigma-Aldrich, St. Louis, MO, USA) added to tap water for 6 or 10 weeks (conventionally called fructose rich diet, FRD 6wk and FRD 10wk, respectively). Food intake and body weight were measured every 48 h. On experimental day, mice were euthanized under non-fasting conditions (08:00 to 09:00 h) and trunk blood was collected; plasma samples were then frozen (– 20°C) until metabolite measurements. Inguinal AT (IAT, subcutaneous depot), Epididymal AT (EAT, visceral depot) and Retroperitoneal AT (RPAT, visceral depot) were aseptically dissected and weighed. EAT was kept in sterile Dulbecco's Modified Eagle's Medium-Low Glucose (1 g/L) (DMEM-LG) for further procedures. Animals were euthanized according to protocols for animal use, in agreement with NIH guidelines for the care and use of experimental animals. All experiments were approved by our Institutional Animal Care Committee.

2.2. Peripheral metabolite measurements

Plasma levels of leptin (Lep) were determined by specific radioimmunoassays (RIAs) previously developed in our laboratory [24]. Circulating glucose (Glu), triacylglycerol (Tg), aspartate aminotransferase (AST), and alanine aminotransferase (ALT) levels were measured using commercial kits (Wiener Lab., Rosario, Argentina).

2.3. EAT stromal vascular fraction cells and adipocytes isolation

Fresh EAT pads were dissected, weighed and digested with collagenase as previously reported [25]. Briefly, fat tissue was minced and digested using 1 mg/mL collagenase solution in DMEM-LG (at 37ºC, for 1h). After centrifugation (1,000 rpm, during 15 min), floating mature adipocytes on the top were separated [25,26] and washed with DMEM-LG 1% BSA (x3). Then adipocytes were resuspended in DMEM-LG-1% BSA for later experiments. Precipitated SVF at the bottom of the tube were separately collected, filtered (in a 50 µm mesh nylon cloth) and washed with DMEM-LG (x3). SVF cells were then resuspended in DMEM-LG supplemented with 10% (v/v) fetal bovine serum (FBS), HEPES (20 nM), 100 IU/mL penicillin, and 100 µg/mL streptomycin (basal medium) and reserved for further measurements.

2.4. Adipocyte culture

Adipocytes were diluted up to a density of approximately 200,000 cells in DMEM-LG-1% BSA and distributed in 24 multi-well plates. For leptin quantification, cells were incubated for 45 min at 37°C in 5% CO2 atmosphere [27] and the medium was carefully aspirated and kept

frozen (-20°C) until measurement as described in section 2.9. Additionally, another set of adipocytes was incubated overnight (ON) under basal conditions (DMEM-LG-1% BSA) or in presence of LPS (DMEM-LG-1% BSA supplemented with 100ng/ml LPS) for further measurement of IL-6 in the supernatants by ELISA (BD OptEIA IL-6).

2.5. Histology

For EAT histological studies, freshly dissected EAT pads were fixed in 4% paraformaldehyde, then washed with tap water, immersed in a series of graded ethanol (70, 96 and 100%), and clarified in xylene before paraffin embedding [28]. Four-micrometer sections were taken from different levels of the blocks and stained with hematoxylin-eosin. Quantitative morphometric analysis was performed using a RGB CCD Sony camera and the automated Open Source software Adiposoft as a plug-in for Fiji software [29](magnification, x400). For each tissue sample, seven sections and three levels were selected. Systematic random sampling was used to select 15 fields for each section, and 2,500 cells per group were examined. Adipocyte area was measured [30].

For histological liver study, fresh samples were fixed in 4% paraformaldehyde for 24 h. Then, they were immersed in different ethanol concentrations (96 and 100%) followed by xylene incubation. Finally, livers were embedded in paraffin, 5-6 µm sections were taken from different levels of the block and then stained with hematoxylin-eosin. Representative images were taken using a RGB CCD Sony camera.

2.6. Glucose tolerance test (GTT).

Four days before the end of the protocols, the experimental groups were fasted overnight and then glucose (2 mg/kg BW) was injected i.p. Blood was collected by the tail cut method. Glucose was measured at 0, 30, 60 and 120 min after glucose challenge using a one-touch glucometer (Accu-Chek Performa). Area under the curve was calculated using Graph Pad Prism 6.0.

2.7. Liver lipid content

Fifty mg of liver was homogenized in 500 µL of 5% solution of Triton X-100 in PBS. The homogenate was incubated at 80-100°C for 5 min and centrifuged at 10,000 g for 10 min. Tg was measured in the supernatants using a commercial kit (Wiener Lab, Rosario, Argentina).

2.8. RNA isolation and quantitative Real-Time PCR (qRT-PCR)

Total RNA was isolated from cells by the Trizol extraction method (Invitrogen, Life Tech., USA) and reverse-transcribed using random primers (250 ng) and RevertAid Reverse Transcriptase (200 U/ul, Thermo Scientific, Lithuania). Two µL cDNA were amplified with HOT FIRE Pol EvaGreenqPCR Mix Plus (Solis BioDyne, Estonia) containing 0.5 µM of each specific primer, using a Rotor Gene Q (Qiagen, Hilden, Germany). PCR efficiency was near 1. Expression levels were analyzed for β-actin (ACTβ, reporter gene), Adiponectin (Adipo), Leptin (Ob), Tumor Necrosis Factor α (TNFα), Interleukin 1β (IL-1β), Interleukin 6 (IL-6), Interleukin 10 (IL-10), and mannose receptor (CD206). Designed primers are shown in Table 1. Relative changes in the expression level of one specific gene were calculated by the ΔΔCt method.

2.9. Culture medium measurement

Medium leptin concentration was determined by specific RIA [26]. In this assay, the standard curve ranged between 50 and 12,500 pg/mL, with intra- and inter-assay variation coefficients of 4-6 and 5-8 %, respectively. IL-6 in culture medium was measured following the instructions of the manufacturer (BD OptEIA IL-6). The curve ranged from 16 pg/ml to 1000 pg/ml.

2.10. Flow cytometry analysis

SVF was prepared as reported above. Cell suspensions were then filtered through a 70-µm cell strainer and cells were stained after Fc blocking. Directly fluorochrome-conjugated anti-mouse antibodies or the respective isotype control were used for specific immunostainings (1:50-100 dilutions). For myeloid analysis anti-CD11b (M1/70, BDPharmigen cat#550993), anti-CD11c (HL3, BD cat# 557401), anti-CD206 (C068C2, BioLegend) anti-Ly6C (AL-21, BD cat#553104) were used. Cells were analyzed in a FACS Calibur flow cytometer (BD bioscience). Analysis was performed using CellQuest Pro (Becton-Dickinson, San Jose, CA, USA) and FlowJo software (TreeStar, San Carlo, CA, USA).

2.11. Adipocytes and monocyte cell line (RAW264.7) co-culture

Direct co-cultures were performed by adding adipocytes from EAT ($2x10^5$cells) to 24-well plates containing RAW264.7 cells (8×10^4cells, monocytes cell line) in DMEM-LG 1% FBS ON. Adipocytes remained floating, forming a cell top layer in the culture well, avoiding direct contact with RAW cells. Then, adipocytes were removed and RAW264.7 culture was washed with Hank's solution (x5). DMEM-LG medium from co-culture was stored at -80ºC for IL-6 ELISA analysis. Then, RAW264.7 cells were divided into three groups depending on the stimulus they received: control medium alone (DMEM-LG 10% FBS), control medium supplemented with LPS

(100 ng/ml) or control medium supplemented with IL-4 (10 ng/ml) for 6 h. Finally, total RNA was extracted from RAW264.7 cells and processed for qPCR quantification of pro-inflammatory (IL-6) or anti-inflammatory (CD206) markers.

2.12. Statistical analysis

Results are expressed as mean values ± SD. Metabolic parameters and flow cytometry studies were analyzed by ANOVA (two-way) with Tukey's multiple comparison test. For the GTT a two-way ANOVA with repeated measures (mixed model) was performed. In vitro studies were analyzed by ANOVA (one-way) with Tukey's multiple comparison test. P values lower than 0.05 were considered statistically significant. All statistical tests were performed using GraphPad Prism 6.0 (GraphPad Software Inc., San Diego, CA, USA).

3. Results

3.1. Metabolic effects of FRD

In a recent work, we showed the effect 6-week FRD on several metabolic parameters in Swiss mice [31]. In this study we compared them with longer periods of fructose consumption (10 weeks, 10wk) that generated a larger deleterious effect in some of them. Moreover, we continued this study analyzing the inflammatory profile of AT in both periods.

Although FRD mice consumed less food than CTR mice (CTR: 3.05 ± 0.32 gr/mice/day vs. FRD: 2.13 ± 0.31 gr/mice/day; P≤0.003), they were on a hypercaloric diet from 3 to 10 weeks of the experiment due to the calories provided by fructose (FRD: calories from Chow: 5.44 ± 0.52 Kcal/mice/day plus calories from fructose: 6.31 ± 0.54 kcal/mice/day vs. CTR: 8.77 ± 0.78kcal/mice/day). Thus, they showed a significant increase in body weight compared to CTR littermates from fifth week (Fig. 1A, B). Briefly, the metabolic profile of FRD mice was deteriorated by fructose consumption in both periods, evidenced by the increase in plasma Tg and Lep levels; nevertheless, no changes in basal Glu levels were observed (Fig. 1D,E,F). Of notice, after 10 weeks of FRD Lep levels were significantly higher than in FRD 6wk group.

Moreover, when FRD mice were subjected to a GTT, both FRD groups showed an altered glucose management evidenced in the glucose curve and the AUC, indicating an impairment in insulin sensitivity in peripheral tissues (Fig. 1C). Even there was not a significant difference between the periods, after 10 weeks the AUC was higher than after 6 weeks.

3.2. FRD consumption affected AT and liver functionality

As previously shown, FRD produced an increase in the mass of AT depots. After 6 weeks only EAT was significantly increased [31]. Interestingly, after 10 weeks of FRD a significant increase in EAT and IAT mass was evidenced (Fig. 2 A, B), showing the deleterious effect of long periods of fructose intake. For RPAT no differences were observed at any period studied (Fig. 2C). For further studies of AT, we focused on EAT as it showed the most evident increase in AT mass for both periods, and because it is known to be metabolically more active than subcutaneous AT and harbor more immune cells [32]. EAT mass expansion in FRD mice was accompanied by an increase in adipocyte size (Fig. 2D), indicating that the nature of EAT expansion caused by fructose ingestion was mainly hypertrophic. Even more, as fructose consumption periods were extended, hypertrophy got worse and the adipocytes area after FRD 10wk was significantly larger compared to that of FRD 6wk (Fig. 2E). No differences in CTR adipocytes area were found for all timings studied. When we analyzed adipocyte functionality by measuring Lep release during adipocytes culture, we found that FRD adipocytes released higher amounts of Lep into the culture medium than CTR adipocytes (Fig. 2F) and, as observed for plasma Lep, amounts were significantly higher after 10 than 6 weeks of FRD. Regarding, metabolic mRNA expression, ob was higher in EAT from FRD 6wk and 10wk mice and no differences were observed for the periods analyzed. *Adipo* gene expression showed no differences after 6 weeks of FRD compared to CTR. Contrarily, after 10 weeks of FRD a significant decrease in its expression was detected (Fig. 2G).

Finally, we evaluated the liver status after the different periods of fructose intake. We assessed the liver metabolic enzyme levels (ALT and AST) that are surrogate markers used to assess liver damage. In our model, ALT levels were significantly increased only after 10 weeks of FRD (Fig 3A) whereas AST remained unchanged, indicating some liver impairment after a longer period of FRD. Then, we continued studying the triglycerides liver content and observed an increase in FRD-fed mice groups compared to CTR (Fig. 3B). Interestingly, FRD 10wk group showed almost twice-fold liver TG compared with the 6wk counterpart. Moreover, the liver histology showed some parenchymatous degeneration of hepatocytes for both FRD periods studied (ballooning) and some foci of lipid accumulation after 10 weeks (Fig. 3C). Overall, these results indicate that longer periods of FRD altered many metabolic parameters causing AT hypertrophy and affecting the liver histology and functionality.

3.3. FRD favored pro-inflammatory profile (mRNA and M1 subtypes) and reduced anti-inflammatory phenotype (mRNA and M2 macrophages) in EAT

mRNA expression of inflammatory and anti-inflammatory markers was then assessed in AT. We observed that pro-inflammatory markers IL-6 and TNFα were significantly high for both periods of FRD, but IL-1β was significantly higher only after 10wk (Fig. 4A). Anti-inflammatory markers showed a reduction in CD206 and IL-10 being significant after 6wk in the case of CD206 and after 10wk in the case of IL-10 (Fig. 4B). These results indicated a reduction in the anti-inflammatory profile of M2 ATM in the EAT.

Most studies and reviews have assessed macrophages activation in different tissues during obesity, but detailed information about the different populations during the progression of the disease is scarce. Thus, we studied the adipose tissue monocyte-derived macrophages ($CD11b^+$, $Ly6C^+$) by flow cytometry from the SVF of EAT after the two different periods of FRD. We observed a significant increase of this population only after 10 weeks (Fig. 5A,B), indicating a higher recruitment of monocytes from blood. When separated by $Ly6C^{high}$ (phagocytosis and pro-inflammatory) or $Ly6C^{middle}$ (pro-inflammatory) we observed a significant increase in the percentage of the latter population for both periods studied, but the $Ly6C^{high}$ population was significantly larger after 10 weeks of FRD indicating a higher AT inflammatory status as the fructose exposure increased.

Then, we continued studying the pro-inflammatory marker CD11c of adipose tissue macrophages (ATM). Figure 5 C, D shows a significant increase in $Ly6C^+$ and $Ly6C^-$ M1 macrophages compared to controls. Interestingly, the proportion of $Ly6C^-$M1 macrophages was higher than that of $Ly6C^+$ M1. As $Ly6C^-$ macrophages are principally considered tissue resident, these cells may be activated prior to the arrival of classical macrophages or negativized in the tissue after a certain time in it. To our surprise no differences were observed between the treatments tested.

M1 macrophages can be divided into two subtypes: M1a and M1b, depending on the expression of CD206. Even though this marker is commonly used for M2 macrophages determination, M1b macrophages have been found to express this receptor [20]. When specifically different M1 subtypes were evaluated, interesting results were observed. We separated them into four different populations regarding if they expressed $Ly6C^+$ or $CD206^+$ or not. For the M1b ($Ly6C^{+/-}$) ATM no differences were observed after FRD 6wk; only after 10wk (Fig. 5, E) treatment there was a significant increase in this population independently of Ly6C. For M1a ($Ly6C^{+/-}$) ATM the percentage was increased compared to CTR for both periods studied. Of notice, M1a population was larger than that of M1b, and $Ly6C^-$ M1a ATMs were the most increased. Considering literature and results from this study we can hypothesize that

M1b population may show a different activation kinetics than M1a, which is triggered after a proinflammatory environmental exposure and participates in tissue remodeling [33].

On the other hand, we found that the M2 anti-inflammatory ATM population ($CD11b^+$, $CD206^+$, $CD11c^-$) decreased immediately after 6wk of FRD and continued low after 10wk (Fig. 5F). When separated between $Ly6C^{+/-}$ ATMs, we did not find any change in $Ly6C^+$ M2 ATMs population for both periods studied (Fig. 5D). Moreover, its proportion/percentage was noticeably low. $Ly6C^-$ M2 ATMs was the most numerous population but significantly decreased after FRD (6 and 10wk) representing the resident ATMs population.

3.4. Macrophage activation by adipocytes *in vitro*

In order to assess the capacity of adipocytes to produce IL-6 after FRD, mature adipocytes were cultured ON with and without LPS stimulation. IL-6 release was measured by ELISA in the culture medium (Fig. 6A). After 6 weeks of FRD we observed that FRD and CTR LPS adipocytes released slightly higher amounts of IL-6 compared to CTR adipocytes, though values were not significant. Notably, adipocytes from FRD 6wk group significantly increased IL-6 release after stimulation with LPS compared to the other groups. On the other hand, after 10 weeks of FRD we observed that FRD adipocytes under basal conditions already produced significantly higher amounts of IL-6 compared to CTR adipocytes. When adipocytes were stimulated with LPS a higher release of IL-6 was observed for both groups but FRD LPS adipocytes produced the highest amount, significantly different compared to all the other groups. Of notice, FRD 10wk adipocytes under basal conditions or after LPS stimulation from 10wk group produced higher IL-6 than their counterparts from 6wk groups. Thus, FRD adipocytes increase their IL-6 release as time of fructose consumption extends, probably favoring the worsening of the disease and contributing to the AT hypertrophy.

Finally, with the aim of assessing whether adipocytes were capable of imprinting monocytes prior to stimulation with LPS (induction to M1) or IL-4 (M2) we co-cultured adipocytes and RAW264.7 monocytes ON and then monocytes were stimulated or not with LPS or IL4.

First, when co-culture was analyzed without any extra stimulation (LPS or IL4), CD206 (M2 anti-inflammatory ATM marker) was unchanged compared to monocytes without adipocytes (RAW; Data not shown). When mRNA for IL-6 was measured in monocytes co-cultured with adipocytes from CTR or FRD 6wk, it had similar expression to that in monocytes alone (Fig. 6C). On the contrary, adipocytes from FRD 10wk co-cultured with monocytes induced a significant increase in monocyte IL-6 mRNA compared to monocytes alone. IL-6 released by adipocytes and monocytes was also measured in the co-culture medium and was in line with that

observed in the mRNA (Fig 6 D). Briefly, IL-6 was not detected in monocytes cultured alone. When monocytes were co-cultured with CTR or FRD 6wk adipocytes no differences were observed between them but the co-culture with FRD 10wk adipocytes produced a significant increase of IL-6 compared to all the other groups. IL-6 release by co-culture of CTR 10wk was similar to CTR/FRD 6wk. Thus, chronic or longer period of fructose consumption induced a higher proinflammatory environment of AT.

After the co-culture, when monocytes were stimulated with IL4, we analyzed CD206 mRNA expression (Fig. 6E). Surprisingly neither CTR nor FRD adipocytes from 6wk or 10wk groups maintained M2 ATM phenotype. Even though all the groups stimulated with IL4 were significantly lower than the monocytes stimulated without adipocytes co-cultured, we observed that FRD adipocytes markedly reduced the expression of CD206 when compared to CTR counterparts.

Finally, when monocytes were stimulated with LPS after co-culture with 6wk CTR or FRD adipocytes, we observed that monocytes had IL-6 mRNA expression similar to that of LPS monocytes without adipocytes (Fig. 6F). Surprisingly, when monocytes were co-cultured with FRD 10wk adipocytes and stimulated with LPS, it resulted in higher expression of IL-6, though it was not so for CTR 10wk adipocytes co-culture. The latter expression was similar to that of RAW LPS group. The increased expression of IL-6 in LPS stimulated monocytes co-cultured with FRD 10wk adipocytes was significantly different than that of the other groups. These results may indicate that FRD adipocytes favored the M1 ATM phenotype and prevented M2 ATM in EAT principally after 10wk of fructose consumption.

Discussion

Obesity is usually accompanied with AT expansion, particularly visceral, which has been associated with the onset of metabolic disorders [12,34]. The present study shows that high fructose intake in mice induces the metabolic and inflammatory altered profile characteristic of obesity. When we compared the different FRD periods, the longest fructose intake period induced the highest detrimental metabolic effects. FRD-induced obesity is associated to the hypertrophic expansion of AT, characterized by the altered secretion pattern of adipokines that in turn contribute to the development of metabolic disorders and inflammation mediated by macrophages. In this sense, we found low adiponectin mRNA levels after 10 weeks, which may favor the development of insulin resistance and promotion of inflammatory macrophages since adiponectin is known to work as insulin sensitizer and to promote M2 macrophages

[35,36]. Moreover, the higher increase of adipocyte size (hypertrophy) found in FRD 10wk may be related with the increase in leptin (plasma and release *in vitro)* and IL-6 secretion (spontaneously and LPS-induced) by adipocytes [37–41]. This leptin increase observed in obese FRD mice may favor the release of pro-inflammatory cytokines by macrophages and adipocytes, also favoring the development of insulin resistance (impaired insulin action on adipocytes) and may at the same time inhibit the adipogenic process that contributes adipocyte hypertrophy [42–44]. On the other hand, high leptin may also affect lipid deposition in the liver [45]. As we observed for the longest FRD period, the liver functionality was affected by the increase of liver Tg, hepatic ALT transaminase, and histological foci of lipid droplets. Although the deleterious effects of fructose diet are milder when compared to high fat diet, we and many other authors observed that obesity by chronic fructose intake induced metabolic disorders that got worse when time of consumption was extended [12,13,31,46].

In agreement with other reports, we also found an increase in inflammatory markers (IL-6, IL-1β and TNFα) and a decrease in anti-inflammatory markers (CD206: M2 marker and IL-10) in EAT from FRD mice [31,47–50]. Moreover, adipocytes isolated from FRD mice showed an inflammatory response (higher IL-6 release) that worsened when the obese phenotype was more evident (FRD 10 weeks).

ATMs are the most abundant immune cells in AT and play a key role in the physiology and pathophysiology of this tissue [16,19]. M2 ATMs maintain AT homeostasis secreting IL-10 that contributes to insulin sensitivity and inhibition of lipolytic activity [51]. Several studies have shown that when the AT expands, changes in ATMs number and polarization to M1 profile occur [14,52]. This activation has been linked to the development of the metabolic disorders associated with obesity and insulin resistance [53–55]. It is important to notice that studies on rodents have been usually conducted using high-fat diets, but there is little information about inflammation in obese mice induced by fructose rich diets.

$Ly6C^+$ monocytes may be precursors of $Ly6C^-$ monocytes and differentiate into macrophages according to the cellular context [56]. There is probably no clear-cut into M1-versus-M2 states, but rather a dynamic continuum of the M1-M2 spectrum depending on the local cytokine microenvironment. To our knowledge, there are no studies that have used Ly6C expression to identify the different ATM populations during AT expansion induced by a hypercaloric diet. We only found two reports in which Ly6C marker was used to analyze macrophages in spleen and lung [57,58]. Interestingly, when $CD11b^+Ly6C^+$ cells were divided into $Ly6C^{high}$ and $Ly6C^{middle}$, the first subset was significantly increased only after 10 weeks while the second one was

increased after both periods studied. It is known that Ly6C^{middle} has pro-inflammatory profile that could contribute to the AT hypertrophy after both periods analyzed in this work. Moreover, Ly6C^{high} ATMs has high phagocytosis capacity and produces pro-inflammatory cytokines that may favor the worsening of the disease [18].

Then, when we identified activated ATMs expressing Ly6C or not, we observed an increase in the M1 ATMs in EAT from FRD mice. Surprisingly, we found that Ly6C$^-$ M1 ATMs were more abundant than the Ly6C$^+$ counterpart although both were increased during FRD intake. All this may indicate that many ATMs suffered polarization due to the inflammatory environment and this was also observed in formerly obese mice by Zamarron et al. [59]. Regarding M2 ATMs, FRD induced a decrease in Ly6C$^-$ M2 and did not modify Ly6C$^+$ M2, being the first ones the predominant population, usually defined as resident ATMs. This is consistent with the literature that defines tissue resident macrophages that derive from non-classical Ly6C$^-$ monocytes [18,19,44]. Overall, obesity by FRD increased the M1/M2 ATMs ratio, in agreement with what has been described for obese mice under high fat diet, though we included the Ly6C marker analysis in our study [33].

As mentioned above, M1 macrophages are divided into two subsets according to the presence of mannose receptor: M1a (CD11c$^+$CD206$^-$) and M1b (CD11c$^+$CD206$^+$) [18–20]. In the present work we were able to analyze M1a and M1b ATMs and to discriminate the presence or absence of Ly6C in these subsets. Our results indicate that M1a ATMs were activated earlier and remained high at least for the periods studied; on the contrary, M1b ATMs only increased after the longest FRD period. Our results show that Ly6C$^-$ M1a ATMs were found in greater proportion than the Ly6C$^+$ counterpart. Probably, Ly6C$^-$ M1a ATMs derived from resident ATMs that polarized to inflammatory phenotype or Ly6C$^+$ monocytes that dropped the marker during differentiation. M1b subset only increased in FRD 10wk mice, similar to what was found for humans by Nakijama in 2016 (CD11c$^+$ and CD163$^+$)[60]. This latter population seemed to activate after longer periods of inflammation and might be involved in tissue remodeling; however, further studies should be developed to evaluate their particular function [33].

The paracrine interaction between adipocyte and immune cells is extremely complex and plays a key role in AT homeostasis. In steady state adipokines secreted by adipocytes contribute to maintain resident type 2 immune cells. In turn, these cells will maintain insulin sensitivity, browning capacity, normal pattern of adipokine secretion, and adipogenesis creating a virtuous cycle for the organism [35,61,62]. Several studies have used adipocyte-macrophage co-culture to assess their interaction [14,22,63,64], most of them carried out with *in vitro*

differentiated adipocytes from mice or humans, or differentiated adipocytes from cell lines. Our study was performed with EAT mature adipocytes from CTR or FRD mice. We demonstrated that FRD 10wk adipocytes *per se* were able to imprint monocytes toward a M1 phenotype and even more when LPS was added, compared to CTR and FRD 6wk. These results are largely coincident with a recent report by Boutens et al. which shows that preincubation of bone marrow derived macrophages with adipose tissue explant from obese mice favors metabolic and proinflammatory phenotype in macrophages [65]. On the other hand, CD206 expression, an accepted M2 marker, was not modified under basal conditions in any co-culture of our experiments. However, FRD 10wk adipocytes co-culture induced the lowest levels of CD206 after IL4 stimulation. Further studies should be performed to analyze each one contribution. Considering that the recruitment of peripheral monocytes is triggered during AT expansion, our results could indicate that hypertrophic adipocytes facilitate a pro-inflammatory environment that favors M1 ATMs polarization at the expense of M2 ATMs.

Overall, the fructose obesity model detailed in this work showed the worsening of the disease as time of the diet extends. Our model showed the low-grade chronic inflammation, hallmark of obesity, where M1 macrophages were found to play an important role in the disease. Furthermore, M1a and M1b subpopulations were characterized, and M1b increased only after the longest period of FRD. It will be important to determine the role of the latter population, which may worsen the disease being a possible therapeutic blank. The Ly6C marker allowed to better characterize the macrophages population and this may encourage other groups to use it. Finally, hypertrophic adipocytes produce an inflammatory environment that imprint monocytes toward M1 profile which could contribute to the higher M1/M2 ratio observed in obesity.

References

[1] Kabat GC, Kim MY, Chlebowski RT, Vitolins MZ, Wassertheil-Smoller S, Rohan TE. Serum lipids and risk of obesity-related cancers in postmenopausal women. Cancer Causes Control CCC 2017. doi:10.1007/s10552-017-0991-y.

[2] Yadav R, Hama S, Liu Y, Siahmansur T, Schofield J, Syed AA, et al. Effect of Roux-en-Y Bariatric Surgery on Lipoproteins, Insulin Resistance, and Systemic and Vascular Inflammation in Obesity and Diabetes. Front Immunol 2017;8:1512. doi:10.3389/fimmu.2017.01512.

[3] Akinyemiju T, Moore JX, Pisu M, Judd SE, Goodman M, Shikany JM, et al. A Prospective Study of Obesity, Metabolic Health, and Cancer Mortality. Obesity (Silver Spring) 2017. doi:10.1002/oby.22067.

[4] Giovannucci E. Metabolic syndrome, hyperinsulinemia, and colon cancer: a review. Am J Clin Nutr 2007;86:s836-42.

[5] Brochu M, Poehlman ET, Ades PA. Obesity, body fat distribution, and coronary artery disease. J Cardiopulm Rehabil n.d.;20:96–108.

[6] Bray GA. Potential Health Risks From Beverages Containing Fructose Found in Sugar or High-Fructose Corn Syrup. Diabetes Care 2013;36:11–2. doi:10.2337/dc12-1631.

[7] Sloboda DM, Li M, Patel R, Clayton ZE, Yap C, Vickers MH. Early Life Exposure to Fructose and Offspring Phenotype: Implications for Long Term Metabolic Homeostasis. J Obes 2014;2014:1–10. doi:10.1155/2014/203474.

[8] Zubiría MG, Fariña JP, Moreno G, Gagliardino JJ, Spinedi E, Giovambattista A. Excess fructose intake-induced hypertrophic visceral adipose tissue results from unbalanced precursor cell adipogenic signals. FEBS J 2013;280:5864–74. doi:10.1111/febs.12511.

[9] Wozniak SE, Gee LL, Wachtel MS, Frezza EE. Adipose Tissue: The New Endocrine Organ? A Review Article. Dig Dis Sci 2009;54:1847–56. doi:10.1007/s10620-008-0585-3.

[10] Stanhope KL, Schwarz JM, Keim NL, Griffen SC, Bremer AA, Graham JL, et al. Consuming fructose-sweetened, not glucose-sweetened, beverages increases visceral adiposity and lipids and decreases insulin sensitivity in overweight/obese humans. J Clin Invest 2009;119:1322–34. doi:10.1172/JCI37385.

[11] Elliott SS, Keim NL, Stern JS, Teff K, Havel PJ. Fructose, weight gain, and the insulin resistance syndrome. Am J Clin Nutr 2002;76:911–22.

[12] Dekker MJ, Su Q, Baker C, Rutledge AC, Adeli K. Fructose: a highly lipogenic nutrient implicated in insulin resistance, hepatic steatosis, and the metabolic syndrome. Am J Physiol Metab 2010;299:E685–94. doi:10.1152/ajpendo.00283.2010.

[13] Khitan Z, Kim DH. Fructose: A Key Factor in the Development of Metabolic Syndrome and Hypertension. J Nutr Metab 2013;2013:1–12. doi:10.1155/2013/682673.

[14] Lumeng CN, DeYoung SM, Bodzin JL, Saltiel AR. Increased Inflammatory Properties of Adipose Tissue Macrophages Recruited During Diet-Induced Obesity. Diabetes 2007;56:16–23. doi:10.2337/db06-1076.

[15] Shi H, Kokoeva M V, Inouye K, Tzameli I, Yin H, Flier JS. TLR4 links innate immunity and fatty acid-induced insulin resistance. J Clin Invest 2006;116:3015–25. doi:10.1172/JCI28898.

[16] Thomas D, Apovian C. Macrophage functions in lean and obese adipose tissue. Metabolism 2017;72:120–43. doi:10.1016/j.metabol.2017.04.005.

[17] Luche E, Robert V, Cuminetti V, Pomié C, Sastourné-Arrey Q, Waget A, et al. Corrupted adipose tissue endogenous myelopoiesis initiates diet-induced metabolic disease. Elife 2017;6. doi:10.7554/eLife.23194.

[18] Yang J, Zhang L, Yu C, Yang X-F, Wang H. Monocyte and macrophage differentiation: circulation inflammatory monocyte as biomarker for inflammatory diseases. Biomark Res 2014;2:1. doi:10.1186/2050-7771-2-1.

[19] Italiani P, Boraschi D. From Monocytes to M1/M2 Macrophages: Phenotypical vs. Functional Differentiation. Front Immunol 2014;5:514. doi:10.3389/fimmu.2014.00514.

[20] Morris DL, Singer K, Lumeng CN. Adipose tissue macrophages: phenotypic plasticity and diversity in lean and obese states. Curr Opin Clin Nutr Metab Care 2011;14:341–6. doi:10.1097/MCO.0b013e328347970b.

[21] Xie L, Ortega MT, Mora S, Chapes SK. Interactive changes between macrophages and adipocytes. Clin Vaccine Immunol 2010;17:651–9. doi:10.1128/CVI.00494-09.

[22] Keuper M, Dzyakanchuk A, Amrein KE, Wabitsch M, Fischer-Posovszky P. THP-1 Macrophages and SGBS Adipocytes ? A New Human in vitro Model System of Inflamed

Adipose Tissue. Front Endocrinol (Lausanne) 2011;2:89. doi:10.3389/fendo.2011.00089.

[23] Sárvári AK, Doan-Xuan Q-M, Bacsó Z, Csomós I, Balajthy Z, Fésüs L. Interaction of differentiated human adipocytes with macrophages leads to trogocytosis and selective IL-6 secretion. Cell Death Dis 2015;6:e1613. doi:10.1038/cddis.2014.579.

[24] Perelló M, Gaillard RC, Chisari A, Spinedi E. Adrenal enucleation in MSG-damaged hyperleptinemic male rats transiently restores adrenal sensitivity to leptin. Neuroendocrinology 2003;78:176–84. doi:72799.

[25] Giovambattista A, Gaillard RC, Spinedi E. Ghrelin gene-related peptides modulate rat white adiposity. Vitam Horm 2008;77:171–205. doi:10.1016/S0083-6729(06)77008-X.

[26] Giovambattista A, Piermaría J, Suescun MO, Calandra RS, Gaillard RC, Spinedi E, et al. Direct effect of ghrelin on leptin production by cultured rat white adipocytes. Obesity (Silver Spring) 2006;14:19–27. doi:10.1038/oby.2006.4.

[27] Perello M, Castrogiovanni D, Giovambattista A, Gaillard RC, Spinedi E. Impairment in insulin sensitivity after early androgenization in the post-pubertal female rat. Life Sci 2007;80:1792–8. doi:10.1016/j.lfs.2007.02.013.

[28] Alzamendi A, Castrogiovanni D, Gaillard RC, Spinedi E, Giovambattista A. Increased male offspring's risk of metabolic-neuroendocrine dysfunction and overweight after fructose-rich diet intake by the lactating mother. Endocrinology 2010;151:4214–23. doi:10.1210/en.2009-1353.

[29] Galarraga M, Campión J, Muñoz-Barrutia A, Boqué N, Moreno H, Martínez JA, et al. Adiposoft: automated software for the analysis of white adipose tissue cellularity in histological sections. J Lipid Res 2012;53:2791–6. doi:10.1194/jlr.D023788.

[30] Alzamendi A, Del Zotto H, Castrogiovanni D, Romero J, Giovambattista A, Spinedi E. Oral metformin treatment prevents enhanced insulin demand and placental dysfunction in the pregnant rat fed a fructose-rich diet. ISRN Endocrinol 2012;2012:757913. doi:10.5402/2012/757913.

[31] Zubiría M, Gambaro S, Rey M, Carasi P, Serradell M, Giovambattista A. Deleterious Metabolic Effects of High Fructose Intake: The Preventive Effect of Lactobacillus kefiri Administration. Nutrients 2017;9:470. doi:10.3390/nu9050470.

[32] Nosalski R, Guzik TJ. Perivascular adipose tissue inflammation in vascular disease. Br J Pharmacol 2017;174:3496–513. doi:10.1111/bph.13705.

[33] Shaul ME, Bennett G, Strissel KJ, Greenberg AS, Obin MS. Dynamic, M2-like remodeling phenotypes of CD11c+ adipose tissue macrophages during high-fat diet--induced obesity in mice. Diabetes 2010;59:1171–81. doi:10.2337/db09-1402.

[34] Alwahsh SM, Gebhardt R. Dietary fructose as a risk factor for non-alcoholic fatty liver disease (NAFLD). Arch Toxicol 2017;91:1545–63. doi:10.1007/s00204-016-1892-7.

[35] Ohashi K, Parker JL, Ouchi N, Higuchi A, Vita JA, Gokce N, et al. Adiponectin promotes macrophage polarization toward an anti-inflammatory phenotype. J Biol Chem 2010;285:6153–60. doi:10.1074/jbc.M109.088708.

[36] Díez JJ, Iglesias P. The role of the novel adipocyte-derived hormone adiponectin in human disease. Eur J Endocrinol 2003;148:293–300.

[37] Skurk T, Alberti-Huber C, Herder C, Hauner H. Relationship between adipocyte size and adipokine expression and secretion. J Clin Endocrinol Metab 2007;92:1023–33. doi:10.1210/jc.2006-1055.

[38] Wåhlen K, Sjölin E, Löfgren P. Role of fat cell size for plasma leptin in a large population based sample. Exp Clin Endocrinol Diabetes 2011;119:291–4. doi:10.1055/s-0031-1273738.

[39] Cava A La, Matarese G. The weight of leptin in immunity. Nat Rev Immunol 2004;4:371–9. doi:10.1038/nri1350.

[40] Tilg H, Moschen AR. Adipocytokines: mediators linking adipose tissue, inflammation and immunity. Nat Rev Immunol 2006;6:772–83. doi:10.1038/nri1937.

[41] Müller G, Ertl J, Gerl M, Preibisch G. Leptin impairs metabolic actions of insulin in isolated rat adipocytes. J Biol Chem 1997;272:10585–93.

[42] Bai Y, Sun Q. Macrophage recruitment in obese adipose tissue. Obes Rev An Off J Int Assoc Study Obes 2015;16:127–36. doi:10.1111/obr.12242.

[43] Eheim A, Medrikova D, Herzig S. Immune cells and metabolic dysfunction. Semin Immunopathol 2014;36:13–25. doi:10.1007/s00281-013-0403-7.

[44] Guzik TJ, Skiba DS, Touyz RM, Harrison DG. The role of infiltrating immune cells in dysfunctional adipose tissue. Cardiovasc Res 2017;113:1009–23. doi:10.1093/cvr/cvx108.

[45] Lee Y, Yu X, Gonzales F, Mangelsdorf DJ, Wang M-Y, Richardson C, et al. PPAR alpha is

necessary for the lipopenic action of hyperleptinemia on white adipose and liver tissue. Proc Natl Acad Sci U S A 2002;99:11848–53. doi:10.1073/pnas.182420899.

[46] Zubiría M, Alzamendi A, Moreno G, Rey M, Spinedi E, Giovambattista A. Long-Term Fructose Intake Increases Adipogenic Potential: Evidence of Direct Effects of Fructose on Adipocyte Precursor Cells. Nutrients 2016;8:198. doi:10.3390/nu8040198.

[47] Pektas MB, Koca HB, Sadi G, Akar F. Dietary Fructose Activates Insulin Signaling and Inflammation in Adipose Tissue: Modulatory Role of Resveratrol. Biomed Res Int 2016;2016:8014252. doi:10.1155/2016/8014252.

[48] Bargut TCL, Santos LP, Machado DGL, Aguila MB, Mandarim-de-Lacerda CA. Eicosapentaenoic acid (EPA) vs. Docosahexaenoic acid (DHA): Effects in epididymal white adipose tissue of mice fed a high-fructose diet. Prostaglandins, Leukot Essent Fat Acids 2017;123:14–24. doi:10.1016/j.plefa.2017.07.004.

[49] Tsai J, Zhang R, Qiu W, Su Q, Naples M, Adeli K. Inflammatory NF-kappaB activation promotes hepatic apolipoprotein B100 secretion: evidence for a link between hepatic inflammation and lipoprotein production. Am J Physiol Gastrointest Liver Physiol 2009;296:G1287-98. doi:10.1152/ajpgi.90540.2008.

[50] Jang JE, Ko MS, Yun J-Y, Kim M-O, Kim JH, Park HS, et al. Nitric Oxide Produced by Macrophages Inhibits Adipocyte Differentiation and Promotes Profibrogenic Responses in Preadipocytes to Induce Adipose Tissue Fibrosis. Diabetes 2016;65:2516–28. doi:10.2337/db15-1624.

[51] Fujisaka S, Usui I, Bukhari A, Ikutani M, Oya T, Kanatani Y, et al. Regulatory Mechanisms for Adipose Tissue M1 and M2 Macrophages in Diet-Induced Obese Mice. Diabetes 2009;58:2574–82. doi:10.2337/db08-1475.

[52] Wada T, Ishikawa A, Watanabe E, Nakamura Y, Aruga Y, Hasegawa H, et al. Eplerenone prevented obesity-induced inflammasome activation and glucose intolerance. J Endocrinol 2017;235:179–91. doi:10.1530/JOE-17-0351.

[53] Prieur X, Mok CYL, Velagapudi VR, Núñez V, Fuentes L, Montaner D, et al. Differential Lipid Partitioning Between Adipocytes and Tissue Macrophages Modulates Macrophage Lipotoxicity and M2/M1 Polarization in Obese Mice. Diabetes 2011;60:797–809. doi:10.2337/db10-0705.

[54] Odegaard JI, Ricardo-Gonzalez RR, Goforth MH, Morel CR, Subramanian V, Mukundan L,

et al. Macrophage-specific PPARgamma controls alternative activation and improves insulin resistance. Nature 2007;447:1116–20. doi:10.1038/nature05894.

[55] Patsouris D, Li P-P, Thapar D, Chapman J, Olefsky JM, Neels JG. Ablation of CD11c-positive cells normalizes insulin sensitivity in obese insulin resistant animals. Cell Metab 2008;8:301–9. doi:10.1016/j.cmet.2008.08.015.

[56] Arnold L, Henry A, Poron F, Baba-Amer Y, van Rooijen N, Plonquet A, et al. Inflammatory monocytes recruited after skeletal muscle injury switch into antiinflammatory macrophages to support myogenesis. J Exp Med 2007;204:1057–69. doi:10.1084/jem.20070075.

[57] Misharin A V., Morales-Nebreda L, Mutlu GM, Budinger GRS, Perlman H. Flow Cytometric Analysis of Macrophages and Dendritic Cell Subsets in the Mouse Lung. Am J Respir Cell Mol Biol 2013;49:503–10. doi:10.1165/rcmb.2013-0086MA.

[58] Rose S, Misharin A, Perlman H. A novel Ly6C/Ly6G-based strategy to analyze the mouse splenic myeloid compartment. Cytometry A 2012;81:343–50. doi:10.1002/cyto.a.22012.

[59] Zamarron BF, Mergian TA, Cho KW, Martinez-Santibanez G, Luan D, Singer K, et al. Macrophage Proliferation Sustains Adipose Tissue Inflammation in Formerly Obese Mice. Diabetes 2017;66:392–406. doi:10.2337/db16-0500.

[60] Nakajima S, Koh V, Kua L-F, So J, Davide L, Lim KS, et al. Accumulation of CD11c $^{+}$ CD163 $^{+}$ Adipose Tissue Macrophages through Upregulation of Intracellular 11β-HSD1 in Human Obesity. J Immunol 2016;197:3735–45. doi:10.4049/jimmunol.1600895.

[61] Machida K, Okamatsu-Ogura Y, Shin W, Matsuoka S, Tsubota A, Kimura K. Role of macrophages in depot-dependent browning of white adipose tissue. J Physiol Sci 2017. doi:10.1007/s12576-017-0567-3.

[62] Hui X, Gu P, Zhang J, Nie T, Pan Y, Wu D, et al. Adiponectin Enhances Cold-Induced Browning of Subcutaneous Adipose Tissue via Promoting M2 Macrophage Proliferation. Cell Metab 2015;22:279–90. doi:10.1016/j.cmet.2015.06.004.

[63] Lacasa D, Taleb S, Keophiphath M, Miranville A, Clement K. Macrophage-secreted factors impair human adipogenesis: involvement of proinflammatory state in preadipocytes. Endocrinology 2007;148:868–77. doi:10.1210/en.2006-0687.

[64] Constant VA, Gagnon A, Landry A, Sorisky A. Macrophage-conditioned medium inhibits the differentiation of 3T3-L1 and human abdominal preadipocytes. Diabetologia

2006;49:1402–11. doi:10.1007/s00125-006-0253-0.

[65] Boutens L, Hooiveld GJ, Dhingra S, Cramer RA, Netea MG, Stienstra R. Unique metabolic activation of adipose tissue macrophages in obesity promotes inflammatory responses. Diabetologia 2018. doi:10.1007/s00125-017-4526-6.

Table 1. Primers used for real time PCR analysis.

Gene	Sequence (5'-3')	GBAN	Size product (bp)
ACTβ	Fw: TTGCAGCTCCTTCGTTGCC Rv: ACCCATTCCCACCATCACAC	NM_007393.5	189
Ob	Fw: ACCAGGATCAATGACATTTCACAC Rv: GGCTGGTGAGGACCTGTTGA	NM_008493.3	148
Adipo	Fw: GGAACTTGTGCAGGTTGGATG Rv: CCCTTCAGCTCCTGTCATTCC	NM_009605.5	171
TNFα	Fw: ATCTTCTCAAAATTCGAGTGACAA Rv: CCTCCACTTGGTGGTTTGCT	NM_013693.3	63
IL6	Fw: GTTCTCTG GAAATCGTGGAAA Rv: AAGTGCATCATCGTTGTTCATACA	NM_031168.2	77
IL1β	Fw: CTTGTGCAAGTGTCTGAA Rv: AGGTCAAAGGTTTGGAAG	NM_008361.4	143
IL10	Fw: CATTTGAATTCCCTGGGTGAGA Rv: TGCTCCACTGCCTTGCTCTT	NM_010548.2	101
CD206	Fw: GGCTGATTACGAGCAGTGGA Rv: CATCACTCCAGGTGAACCCC	NM_008625.2	90

Figure 1. Mean of caloric intake, body weight and metabolic parameters. A) Caloric intake and (B) body weight. C) GTT was performed four days before to the end of the protocols. Glucose concentration was measured at 0, 30, 60 and 120 minutes after glucose challenge. Area under the curve measured using the graph pad prism 6.0. D) Glucose E) Triglycerides and F) Leptin plasma concentrations were assessed (*P <0.05, ** P <0.01, *** P<0.001 and ****P <0.0001 vs. CTR; +P<0.05 and +++P<0.001 vs. FRD 6wk). Values are mean ± SD (n=10 mice per group).

Figure 2. AT expansion, function and metabolic gene expression along FRD period. A) EAT B) IAT and C) RPAT mass were weighted. D) representative EAT histological samples stained with hematoxylin-eosin and E) EAT adipocyte size. F) Leptin secretion of adipocytes incubated with basal medium. G) EAT mRNA expression of adiponectin (Adipo) and leptin (Lep). *P <0.05, ** P <0.01, ***P <0.001, ****P <0.001 vs. CTR; +P <0.05, ++P <0.01 vs. FRD 6wk. Values are mean ± SD (n=6-8 mice per group).

Figure 3. Liver histology and metabolic parameters along FRD period. A) ALT and AST activity measurement B) Liver triglycerides content C) representative liver histological samples stained with hematoxylin-eosin and D) with higher magnification of the selected area. *P <0.05; ** P<0.01 vs. CTR; +++ P <0.001 vs. FRD 6wk. Values are mean ± SD (n=8-10 mice per group).

Figure 4. Inflammatory markers (mRNA). A) Gene expression of pro-inflammatory cytokines IL6, TNFα and IL1β and B) anti-inflammatory markers, CD206 and IL10, from EAT of CTR and FRD after 6 and 10wk. *P <0.05, **P<0.01 vs. CTR. Values are mean ± SD (n= 6 mice per group).

Figure 5. Flow cytometry analysis of myeloid population in AT along FRD period. A) Representative density plots of ly6C study using SVF cells from EAT of CTR10wk and FRD10wk. B) Quantitative Ly6C expression analyzed by flow cytometry (% to $CD11b^+$ cells) C) representative plots of M1 ATMs and subtypes (M1a and M1b) and M2 ATMs in SVF cells from EAT of CTR10wk and FRD10wk mice. 6 and 10wk CTR and FRD SVF cells quantitative study of

D) M1 ATMs; E) M1a and M1b subtypes (% to $CD11b^+$ cells) and F) M2 ATMs (% to $CD11b^+CD206^+$ cells) expression. *P <0.05, ** P <0.01, ***P <0.001 ****P <0.0001 vs. CTR; +P <0.05; +++P <0.001 vs. FRD 6wk. Values are mean ± SD (n=6-8 mice per group).

Figure 6. Adipocytes IL6 release and co-culture with monocytes cell line (RAW264.7) A) IL6 secretion of adipocytes culture incubated with basal medium or LPS in the different groups. B) *in vitro* experimental set-up of RAW264.7 co-culture with adipocytes ON from CTR or FRD mice followed with 6h monocytes stimulation with LPS (100ng/ml) or IL4 (10ng/ml). C) IL6 mRNA expression of monocytes from co-culture or alone. D) IL6 secretion from co-culture or monocytes alone. E,F). CD206 or IL6 mRNA expression assessed in RAW2064.7 after LPS (100ng/ml) or IL4 (10ng/ml) stimulation, respectively. mRNA samples are referred to monocytes without stimulation. *P <0.05, **P <0.01, ***P<0.001, ****P <0.0001 vs. CTR, #P<0.05,##P<0.01 vs. RAW264.7; +P<0.05, ++P <0.01, +++ P<0.001 and ++++P <0.0001 vs. FRD 6wk, Δ P<0.05 vs. all the groups. Values are mean ± SD (n=6 mice per group).

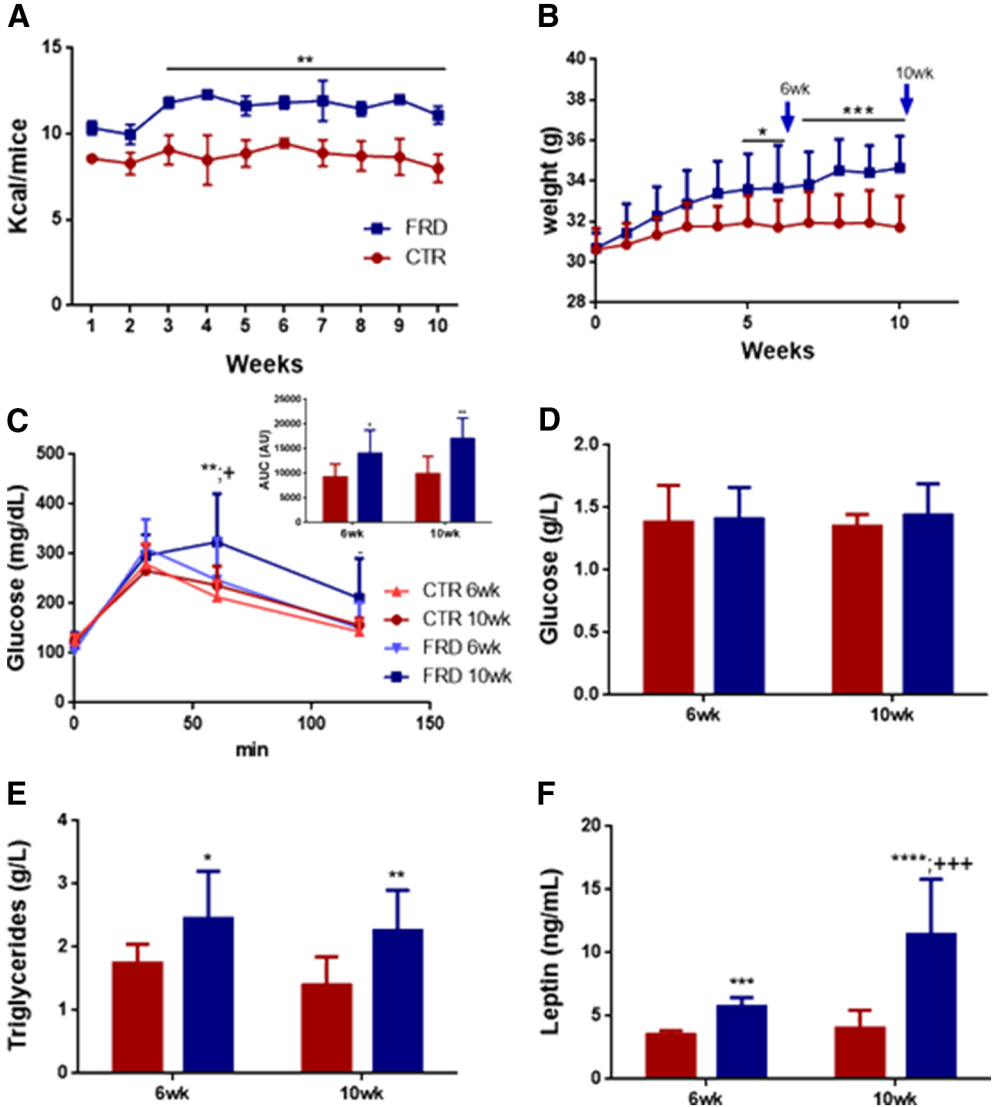
A
Kcal/mice
Weeks
FRD
CTR
B
weight (g)
Weeks
6wk
10wk
C
Glucose (mg/dL)
min
AUC (AU)
CTR 6wk
CTR 10wk
FRD 6wk
FRD 10wk
D
Glucose (g/L)
6wk
10wk
E
Triglycerides (g/L)
6wk
10wk
F
Leptin (ng/mL)
6wk
10wk

Figure 1

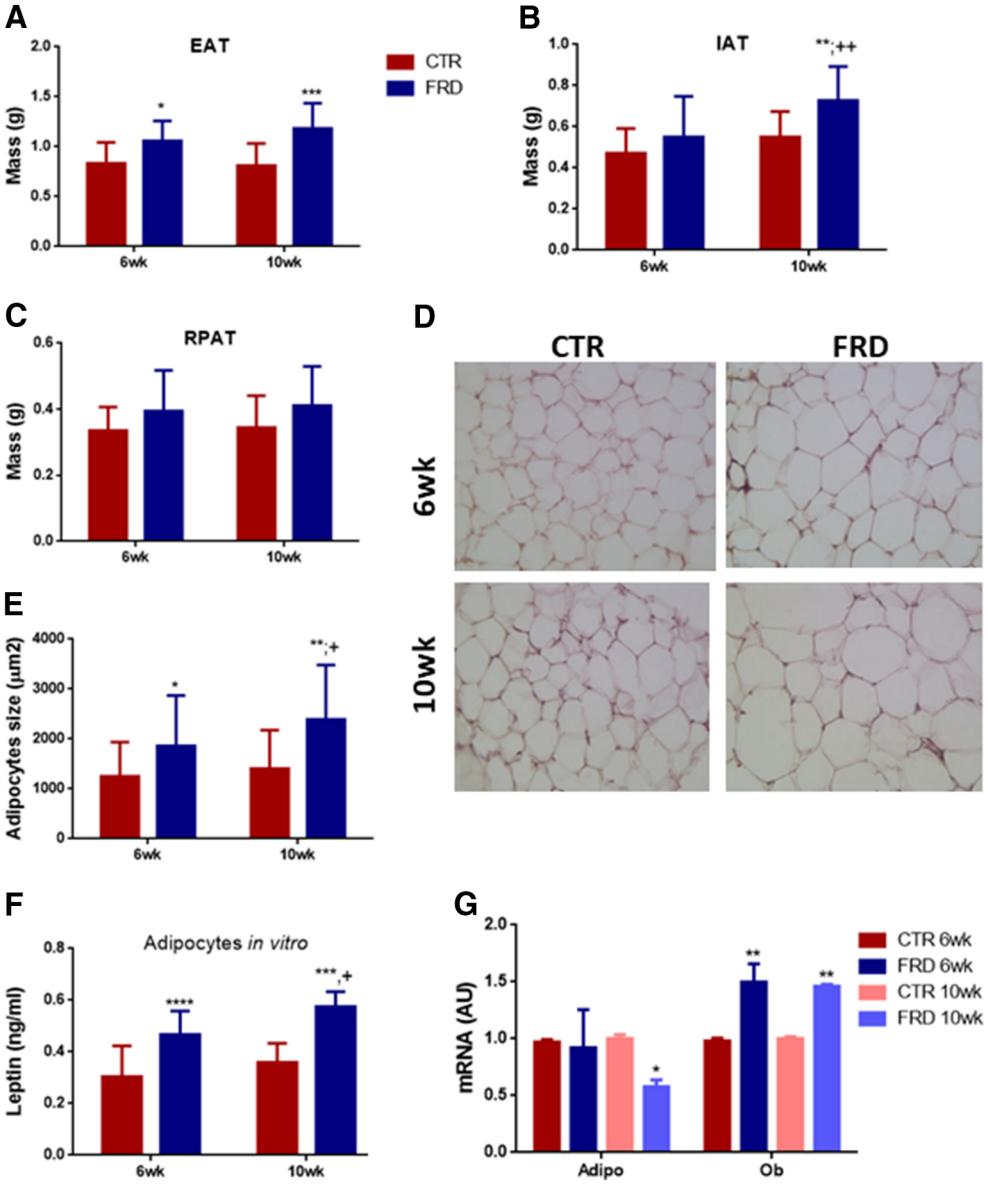
A
EAT
CTR
FRD
Mass (g)
2.0
1.5
1.0
0.5
0.0
*
***
6wk
10wk
B
IAT
**;++
Mass (g)
1.0
0.8
0.6
0.4
0.2
0.0
6wk
10wk
C
RPAT
Mass (g)
0.6
0.4
0.2
0.0
6wk
10wk
D
CTR
FRD
6wk
10wk
E
Adipocytes size (µm2)
4000
3000
2000
1000
0
*
**;+
6wk
10wk
F
Adipocytes in vitro
Leptin (ng/ml)
0.8
0.6
0.4
0.2
0.0
****
***;+
6wk
10wk
G
mRNA (AU)
2.0
1.5
1.0
0.5
0.0
*
**
**
CTR 6wk
FRD 6wk
CTR 10wk
FRD 10wk
Adipo
Ob

Figure 2

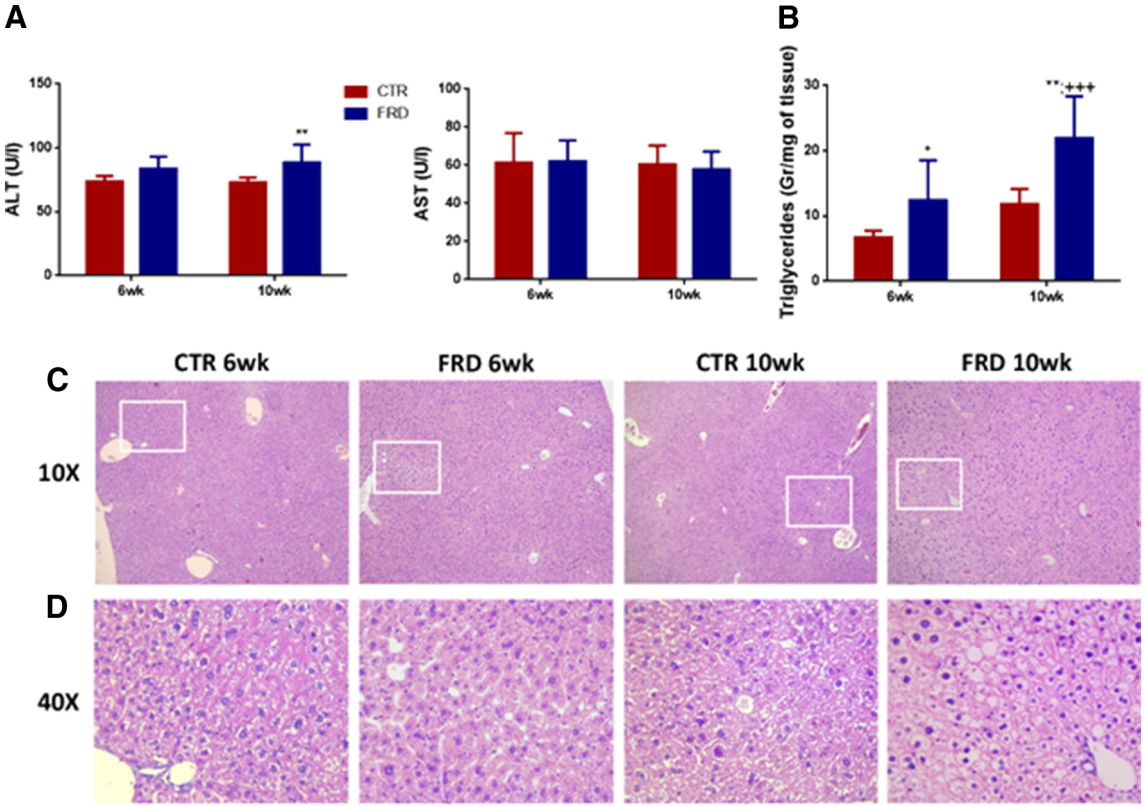
A
ALT (U/l)
150
100
50
0
**
CTR
FRD
6wk
10wk
AST (U/l)
100
80
60
40
20
0
6wk
10wk
B
Triglycerides (Gr/mg of tissue)
30
20
10
0
*
**:+++
6wk
10wk
C
CTR 6wk
FRD 6wk
CTR 10wk
FRD 10wk
10X
D
40X

Figure 3

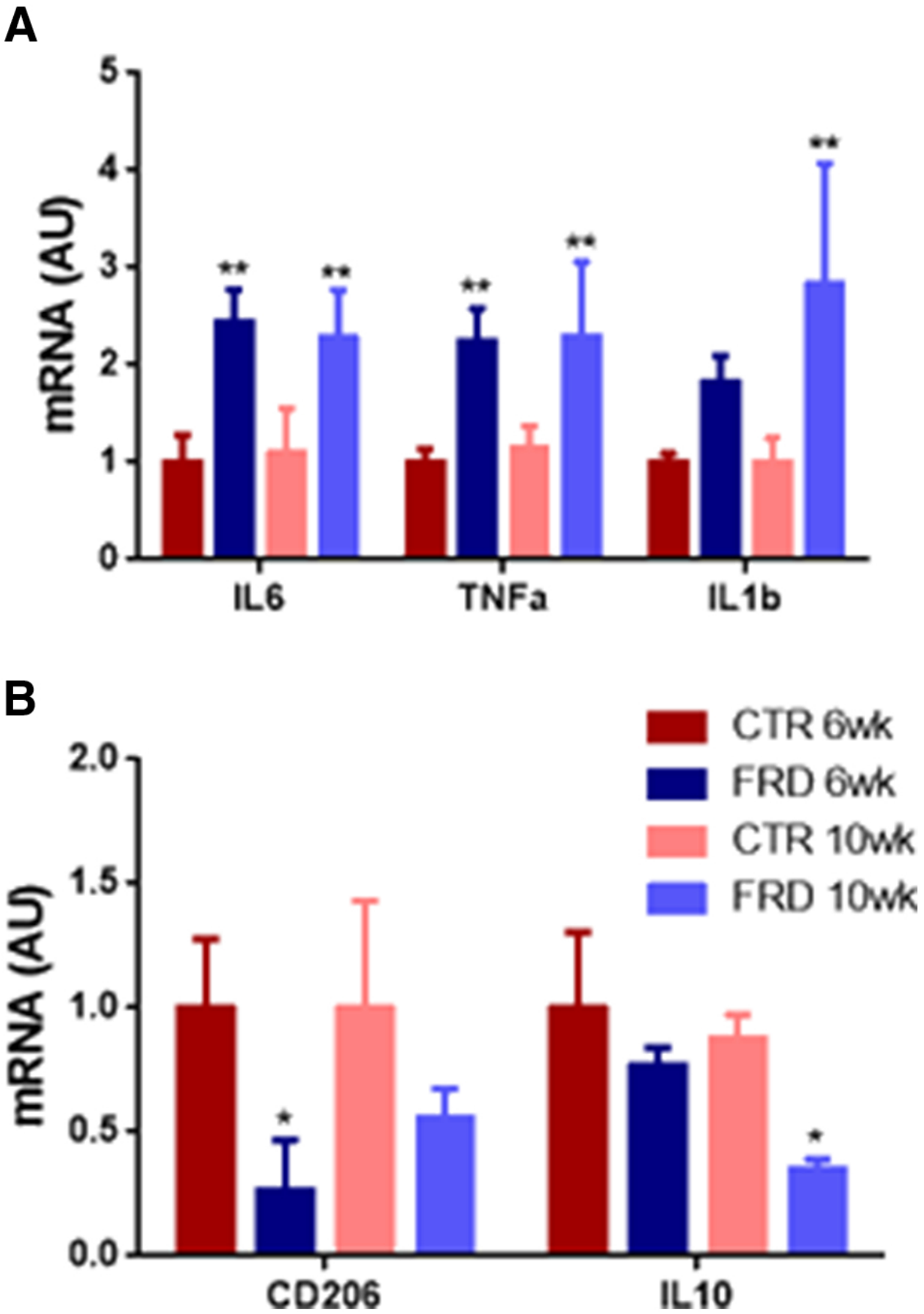
A
mRNA (AU)
0
1
2
3
4
5
**
**
**
**
**
IL6
TNFa
IL1b
B
mRNA (AU)
0.0
0.5
1.0
1.5
2.0
*
*
CD206
IL10
CTR 6wk
FRD 6wk
CTR 10wk
FRD 10wk

Figure 4

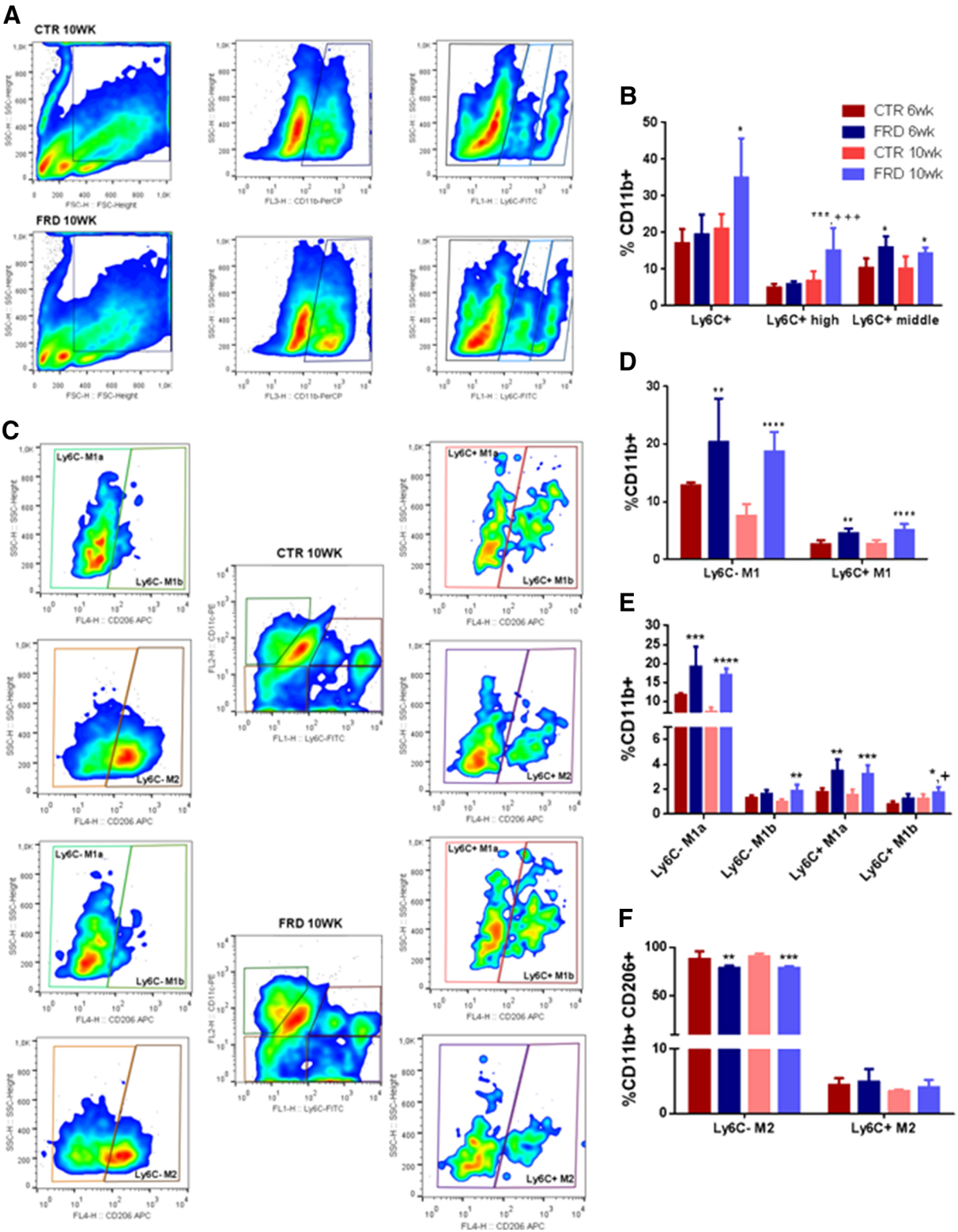
A
CTR 10WK
FRD 10WK
B
CTR 6wk
FRD 6wk
CTR 10wk
FRD 10wk
% CD11b+
Ly6C+
Ly6C+ high
Ly6C+ middle
C
CTR 10WK
FRD 10WK
Ly6C- M1a
Ly6C- M1b
Ly6C- M2
Ly6C+ M1a
Ly6C+ M1b
Ly6C+ M2
D
%CD11b+
Ly6C- M1
Ly6C+ M1
E
%CD11b+
Ly6C- M1a
Ly6C- M1b
Ly6C+ M1a
Ly6C+ M1b
F
%CD11b+ CD206+
Ly6C- M2
Ly6C+ M2

Figure 5

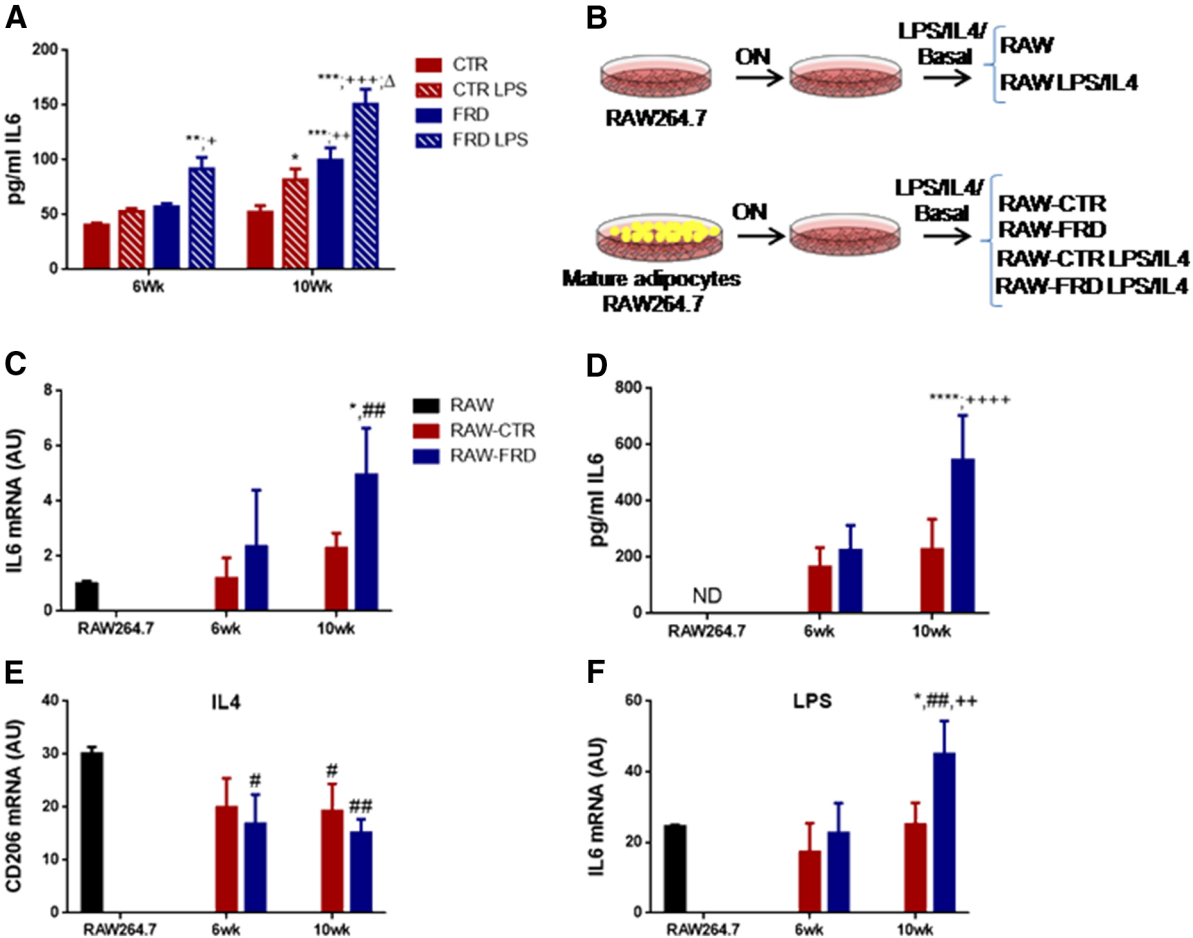
A
pg/ml IL6
CTR
CTR LPS
FRD
FRD LPS
6Wk
10Wk
B
RAW264.7
ON
LPS/IL4/
Basal
RAW
RAW LPS/IL4
Mature adipocytes
RAW264.7
RAW-CTR
RAW-FRD
RAW-CTR LPS/IL4
RAW-FRD LPS/IL4
C
IL6 mRNA (AU)
RAW
RAW-CTR
RAW-FRD
RAW264.7
6wk
10wk
D
pg/ml IL6
ND
E
IL4
CD206 mRNA (AU)
F
LPS
IL6 mRNA (AU)

Figure 6